Stepwise Chromium(II) and Vanadium(II) Reductions of the μ-Amido-μ-superoxo- and μ-Amido-μ-peroxo-bis[bis(ethylenediamine)cobalt(III)] Complexes

By **Michael R. Hyde** and **A. Geoffrey Sykes,*** Department of Inorganic and Structural Chemistry, The University, Leeds LS2 9JT

The five-equivalent Cr^{2+} reduction of the μ-amido-μ-superoxo-complex, $[(en)_2Co{\cdot}\mu(NH_2,O_2){\cdot}Co(en)_2]^{4+}$, has been studied in aqueous perchlorate media, I = 2·0M ($LiClO_4$). Fast outer-sphere reduction to the μ-amido-peroxo-complex $[(en)_2Co{\cdot}\mu(NH_2,O_2){\cdot}Co(en)_2]^{3+}$ is observed in the initial step, $k \geqslant 1{\cdot}4 \times 10^5$ l mol^{-1} s^{-1} at temperatures in the range 4—35 °C. The first stage of reduction of the μ-amido-μ-peroxo-complex is inner sphere and Co^{2+}, but not hexa-aquochromium(III), is obtained following ion-exchange separation of the products of the 1 : 1 reaction. Reaction occurs predominantly *via* the unprotonated form of the complex: k (25 °C) = 2100 ± 60 l mol^{-1} s^{-1}, $\Delta H^{\ddagger}$ = 7·75 ± 0·25 kcal mol^{-1}, and $\Delta S^{\ddagger}$ = −17·5 ± 0·9 cal K^{-1} mol^{-1}. From our observations it is concluded that a mixed μ-peroxo-cobalt(III)–chromium(III) complex $(NH_3)(en)_2Co{\cdot}O_2{\cdot}Cr(H_2O)_5^{4+}$ is formed. Other subsequent stages, some of which are independent of $[Cr^{2+}]$ and involve isomerisation, have been studied and kinetic data obtained. The remaining cobalt(III) chromophore dominates the u.v.–visible spectrum until the peroxo-bridge has been fully reduced to give a μ-hydroxo-cobalt(III)–chromium(III) complex. The latter is reduced in the final slow step which is outer sphere, rate constant (1·09 ± 0·07) × 10^{-3} l mol^{-1} s^{-1} at 35 °C, with no dependence on $[H^+]$ in the range 0·08—0·50M investigated. Less extensive studies on the V^{2+} reduction of the μ-amido-μ-superoxo- and μ-amido-μ-peroxo-complexes are also reported.

REDOX reactions of the μ-amido-μ-superoxo-complex (I) and the μ-amido-μ-peroxo-complex (II) in the ethylenediamine series have been extensively studied in these

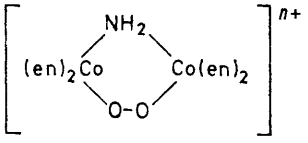

(I) n = 4
(II) n = 3

laboratories.[1,2] Although the structures of (I) and (II) have similar features,[3] their redox behaviour is considerably different.

Much of the available data support an outer-sphere mechanism for reduction of the superoxo-bridging ligand in (I). This is substantiated by reduction of the singly bridged superoxo-complex (III), in which Cr^{2+}, V^{2+}, Eu^{2+},[4] and Fe^{2+} [5] are now believed to reduce (III) by

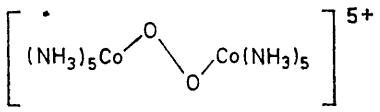

(III)

an outer-sphere mechanism. Reactions of the μ-peroxo-complex (II) proceed in quite a different manner and the products often indicate an inner-sphere mode of attack. The different mechanisms observed for reduction of (I) and (II) are consistent with non-donor and donor properties exhibited by the superoxo- and peroxo-bridges of these complexes.[1]

A detailed study of the five-equivalent Cr^{2+} reduction of (I) is reported. The first equivalent of reductant gives complex (II). Kinetic data for the Cr^{2+} and V^{2+} reductions of isomeric forms of protonated (II) are considered and the different mechanisms which are manifest in the reduction of superoxo-, peroxo-, and hydroperoxo-bridging ligands discussed.

Preliminary investigations indicated a wide range of redox activity for these related binuclear complexes. The superoxo-complex (I) is reduced so rapidly by Cr^{2+} that the rate process cannot be observed on the stopped-flow apparatus, whereas the final stage of reduction of (II) is too slow to follow using the stopped-flow spectrophotometer. Reactions were monitored using the stopped-flow technique and (where necessary) conventional spectrophotometry. Scan spectra were obtained using a Unicam SP 800 spectrophotometer, and in one case from the stopped-flow apparatus.

The Cr^{2+} *Reduction of* μ*-Amido-*μ*-superoxo-complex.*—The reaction was monitored at the absorbance maximum for (I), λ = 687 nm (ε = 485 l mol^{-1} cm^{-1}). With $[Co^{III}_2]$ = 3·9 × 10^{-4}M, $[Cr^{2+}]$ = 2·5 × 10^{-2}M, $[H^+]$ = 0·1M, and the ionic strength I = 2·0M ($LiClO_4$) an absorbance change ΔO.D. = 0·36 was expected. At temperatures of 4·0 and 35·0 °C there was no evidence for an observable rate process using the stopped-flow apparatus. Final absorbance readings indicated complete consumption of (I) within the time of mixing. Assuming total reaction within the time of mixing 2 ms, a half-life for reaction $t_{\frac{1}{2}}$ is estimated at ⩽0·2 ms. The first-order rate constant is accordingly ⩾3·5 × 10^3 s^{-1}, and if the reaction is first order in $[Cr^{2+}]$ the second-order rate constant is ⩾1·4 × 10^5 l mol^{-1} s^{-1} between 3 and 35 °C. Ion-exchange separation of the products of a 1 : 1 reaction are consistent with outer-sphere reduction of the superoxo-bridge (see below). Although the dicobalt(III) product was not isolated the spectrum obtained with a 1 : 1 ratio of reactants was identical to that of the μ-peroxo-complex (II) (see Figure 3 below).

Preliminary Observations on the Cr^{2+} *Reduction of the*

[1] A. G. Sykes, *Chem. in Brit.*, 1974, **10**, 170.
[2] For a recent review on binuclear complexes see A. G. Sykes and J. A. Weil, *Progr. Inorg. Chem.*, 1970, **13**, 1—106.
[3] For details of the structures see U. Thewalt and R. E. Marsh, *Inorg. Chem.*, 1970, **25**, 596; Table 1, p. 6, of reference 2.
[4] A. B. Hoffman and H. Taube, *Inorg. Chem.*, 1968, **7**, 1971.
[5] R. Davies and A. G. Sykes, *J. Chem. Soc.* (*A*), 1968, 2831.

μ-Amido-μ-peroxo-complex.—It has been demonstrated in the previous section that the product of the initial reaction is the μ-amido-μ-peroxo-complex (II). Subsequent stages of the Cr^{2+} reduction were therefore studied using stock solutions of (II). This approach was preferred since (II) is not photochemically active and is stable over much longer periods in neutral solution.[6]

The stepwise reduction of (II) as indicated below is somewhat complicated and certain stages which are observed involve isomerisation/decomposition rather than Cr^{2+} reduction. It is, however, clear that the first and last stages observed correspond to Cr^{2+} reduction of the cobalt(III) centres in the complex, since a cobalt(III) chromophore dominates the visible spectrum up to the final stage of reduction (see Figure 3). Intermediate stages show a more complicated behaviour and the assignments made are less certain.

First Stage of the Cr^{2+} Reduction of the μ-Amido-μ-peroxo-complex.—At ionic strength $I = 0{\cdot}245$M the different protonated and unprotonated forms of the μ-amido-μ-peroxo-complex are well characterised.[7] Conversion of the protonated peroxo-complex into the hydroperoxo-form [(BH) and (AH) respectively], equation (1), is much slower ($k = 0{\cdot}059$ s^{-1} at 25 °C, $I = 0{\cdot}245$M) [7] than the

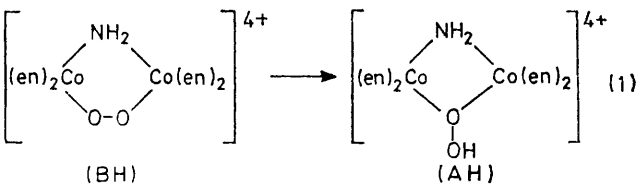

observed redox processes reported here. Since there was no acid present in solutions of the dicobalt(III) complex prior to mixing, it is concluded that there was no AH present in solution.

Absorbance decreases, corresponding to reduction of the dicobalt(III) complex, were monitored on the stopped-flow apparatus at $\lambda = 430$ nm ($\varepsilon = 925$ l mol^{-1} cm^{-1}) for (II). Preliminary runs were carried out with $[Cr^{2+}]$ in 16- to 20-fold excess of $[Co^{III}_2]$, at ionic strength $I = 0{\cdot}245$M, as used by Mori and Weil in earlier work.[7] First-order plots were linear to between 85 and 95% completion. In the range $[H^+] = 0{\cdot}02$—$0{\cdot}209$M a non-linear dependence of second-order rate constant $k_{obs}/[Cr^{2+}]$ upon hydrogen-ion concentration was observed (see Table 1).

TABLE 1

Kinetic data for the first stage Cr^{2+} reduction of the μ-amido-μ-peroxo-complex (B) at 25 °C. $\lambda = 430$ nm, $I = 0{\cdot}245$M ($LiClO_4$). Second-order rate constants are averaged from 3 runs in each case

$[H^+]$ / M	$10^2[Cr^{2+}]$ / M	$10^4[Co^{III}_2]$ / M	$k_{obs}/[Cr^{2+}]$ / l mol^{-1} s^{-1}	$k_{obs}(K_1 + [H^+])$ [a]$/[Cr^{2+}]$ / s^{-1}
0·020	2·04	10·0	464	74·2
0·050	2·01	10·0	369	70·1
0·075	2·03	10·0	339	72·8
0·092	1·62	10·0	325	75·7
0·209	2·00	10·0	215	75·0 [b]

[a] At $I = 0{\cdot}245$M, 25°, $K_1 = 0{\cdot}147$M, ref. 7. [b] $I = 0{\cdot}245$M obtained after mixing solutions of different ionic strengths, 0·478M + 0·012M respectively.

Equilibration of (B), an alternative representation of the 3+ complex (II), and (BH), a 4+ complex is

$$(BH) \overset{K_1}{\rightleftharpoons} (B) + H^+ \qquad (2)$$

rapid and occurs prior to Cr^{2+} reduction. If C_0 is the total concentration of the μ-amido-μ-peroxo-complex and k_2 and k_3 are rate constants for reduction of (B) and (BH) respectively, (3) is obtained, which under pseudo-

$$\frac{-d}{dt}C_0 = [Cr^{2+}]C_0\left(\frac{k_2K_1}{K_1 + [H^+]} + \frac{k_3[H^+]}{K_1 + [H^+]}\right) \qquad (3)$$

first-order conditions gives (4). Using $K_1 = 0{\cdot}14$M [7] at

$$\frac{k_{obs}}{[Cr^{2+}]} = \frac{k_2K_1}{K_1 + [H^+]} + \frac{k_3[H^+]}{K_1 + [H^+]} \qquad (4)$$

25°, $I = 0{\cdot}245$M, the function $k_{obs}(K_1 + [H^+])/[Cr^{2+}]$ shows only a very slight dependence upon $[H^+]$ up to $[H^+] = 0{\cdot}21$M, and it is concluded that $k_3 \ll k_2$.

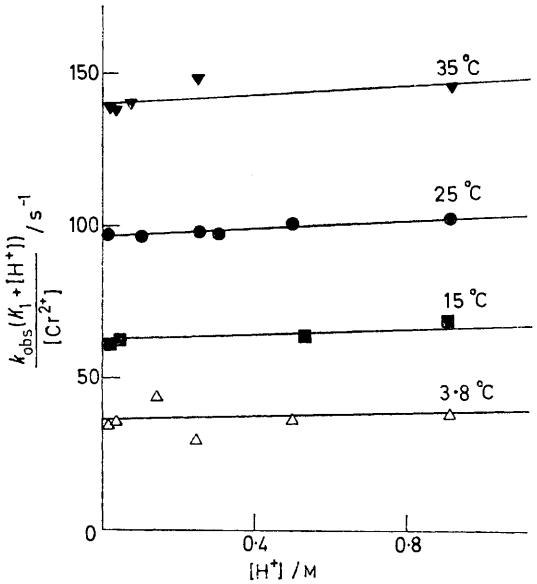

FIGURE 1 The evaluation of k_2 and k_3, equation (4), for the Cr^{2+} reduction of (B) and (BH) respectively, $I = 2{\cdot}0$M ($LiClO_4$). The experimental points are as indicated and the solid lines are as computed using a non-linear least-squares programme

These preliminary runs have now established the mechanism of reaction at $I = 0{\cdot}245$M, and the range of conditions employed have been extended to ionic strength $I = 2{\cdot}0$M ($LiClO_4$) in order that more precise data may be obtained. Absorbance changes were again monitored at $\lambda = 430$ nm using the stopped-flow technique. With $[Cr^{2+}]$ in 13- to 160-fold excess of $[Co^{III}_2]$, pseudo-first-order plots of log (O.D.$_t$ − O.D.$_\infty$) *versus* time were linear for at least 85% reaction. With $[H^+]$ in the range 0·019—0·91M the variation of $k_{obs}/[Cr^{2+}]$ with $[H^+]$ (see Table 2) was similar to that observed at $I = 0{\cdot}245$M. Consequently the same rate expression, equation (3), was used to describe the system (see Figure 1).

[6] R. Davies and A. G. Sykes, *J. Chem. Soc.* (*A*), 1968, 2840.
[7] M. Mori and J. A. Weil, *J. Amer. Chem. Soc.*, 1967, **89**, 3732.

The importance of first defining the rate law at I = 0·245M is apparent since it is necessary to know the relative importance of k_2 and k_3 ($k_2 \gg k_3$) before estimates of K_1 can be made at I = 2·0M ($LiClO_4$).

Once estimates of k_2, k_3, K_1, and the associated activation (and thermodynamic) parameters had been made,

TABLE 2

Kinetic data for the first stage Cr^{2+} reduction of (B), at λ = 430 nm. Ionic strength I = 2·0M ($LiClO_4$). Figures in parentheses indicate the numbers of runs averaged

Temp. °C	$[H^+]$ M	$10^2[Cr^{2+}]$ M	$10^4[Co^{III}_2]$ M	$k_{obs}/[Cr^{2+}]$ l mol^{-1} s^{-1}	
3·8	0·0135	0·50	4·0	539	(2)
	0·0286	1·06	4·0	442	(2)
	0·142	2·69	4·0	228	(2)
	0·250	2·69	4·0	99·0	(2)
	0·500	2·66	4·0	66·0	(2)
	0·920	2·63	4·0	39·0	(2)
15·0	0·0175	0·50	4·0	927	(2)
	0·0350	1·00	4·0	739	(2)
	0·535	2·36	4·0	110	(2)
	0·910	3·00	4·0	72	(2)
25·0	0·019	0·55	4·0	1480	(2)
	0·106	3·03	4·0	636	(2)
	0·250	3·04	4·0	331	(2)
	0·300	3·20	4·0	298	(2)
	0·300	3·20	2·0	296	(2)
	0·300	3·20	8·0	268	(3)
	0·300	0·88	4·0	273	(3)
	0·300	1·65	4·0	271	(3)
	0·300	6·10	4·0	284	(3)
	0·500	3·03	4·0	186	(2)
	0·910	3·03	4·0	108	(2)
35·0	0·0135	0·50	4·0	2420	(2)
	0·0252	0·92	4·0	2010	(2)
	0·070	2·59	4·0	1230	(2)
	0·250	2·69	4·0	505	(1)
	0·920	2·69	4·0	152	(2)

more precise values were obtained (Table 3) using a non-linear least-squares programme,[8] assuming equation (4) to be valid. A weighting factor of $1/y^2$, where $y = k_{obs}/[Cr^{2+}]$, was used throughout.

TABLE 3

Rate constants and activation parameters for the first stage Cr^{2+} reduction of the μ-amido-μ-peroxo-complex at 25 °C, I = 2·0M ($LiClO_4$); K_1, k_2, and k_3 are as defined in equation (4)

	k_2 [a]	k_3 [a]	K_1 [a]
	2100 ± 60	16 ± 6	0·046 ± 0·006
$\Delta H^{\ddagger}$/kcal mol^{-1}	7·75 ± 0·25	5·2 ± 2	−0·9 ± 0·4 [b]
$\Delta S^{\ddagger}$/cal K^{-1} mol^{-1}	−17·5 ± 0·9	−36 ± 7	−9·1 ± 1·3 [b]

[a] Units of k_2, k_3, and K_1 are l mol^{-1} s^{-1}, l mol^{-1} s^{-1}, and mol l^{-1} respectively. [b] Since K_1 is an equilibrium constant ΔH_1 and ΔS_1 are appropriate.

Second Stage of the Cr^{2+} *Reduction of the* μ*-Amido-*μ*-peroxo-complex.*—Once again absorbance decreases were monitored at λ = 430 nm on the stopped-flow apparatus. The first stage of reduction of complex (II) is relatively rapid and does not interfere with the second stage. An intermediate designated (C) is formed in the first stage. First-order plots of log (O.D.$_t$ − O.D.$_\infty$) *versus* time for the further reaction of (C) could not be evaluated directly from stopped-flow traces since a subsequent reaction [the third stage, yielding intermediate (D)] was also operative. These two steps were easily separated by use of standard consecutive reaction treatment, since there was a factor of six between the two rates. A typical example of the separation of two stages is given in Figure 2, where the quantity x used in the insert plot corresponds to the intercept, t = 0, for the main plot. Rate constants k_4, (5), evaluated from runs at 35 °C, I = 2·0M ($LiClO_4$), are independent of $[Cr^{2+}]$ in the range $[Cr^{2+}] = 0.63$ to 5.12×10^{-2}M, and show a direct dependence upon hydrogen-ion concentration for $[H^+]$ = 0·043 to 0·50M (see Table 4). Least-squares analysis (no weighting) of the data in Table 4 gives the rate expression (6). The values of a and b at 35°, I = 2·0M ($LiClO_4$),

$$\frac{-\mathrm{d}}{\mathrm{d}t}[C] = k_4[C] \quad (5)$$

where

$$k_4 = a + b[H^+] \quad (6)$$

are 0·123 + 0·007 s^{-1} and 0·138 ± 0·008 l mol^{-1} s^{-1}, respectively.

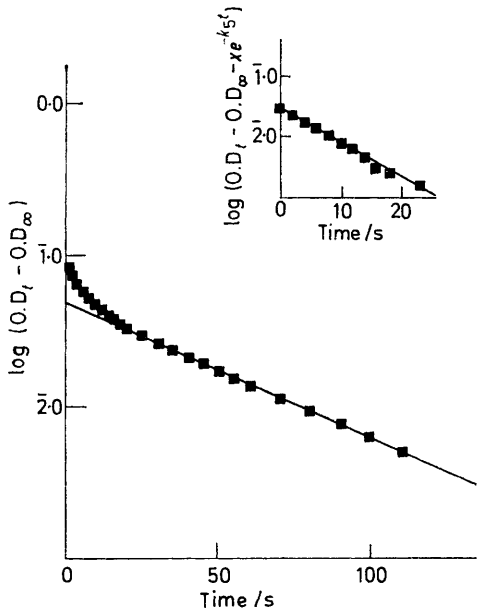

FIGURE 2 Separation of the second and third stages using a consecutive reaction treatment. The gradient in the main figure gives k_5 for the third stage and the insert gives k_4 for the second stage. The reaction was monitored at 430 nm using the stopped-flow technique and the displayed run is entry 8 in Table 4 and entry 7 in Table 5

Data for the two stages, that in the previous section and the above, suggest that the first stage corresponds to Cr^{2+} reduction of the μ-amido-μ-peroxo-complex whereas the second stage is independent of Cr^{2+} and represents some form of isomerisation or decomposition of the intermediate species (C). If this is correct a reaction with just one equivalent of Cr^{2+} per dicobalt(III) complex should also produce a two-stage process, providing the observed first stage is faster than the observed second stage. A reaction was followed at 430 nm, 25 °C, I = 2·0M ($LiClO_4$) with $[Co^{III}_2] = 5.0 \times 10^{-4}$M, $[Cr^{2+}]$ =

[8] Los Alamos Report LA 2367, 1959 and Addenda by R. H. Moore and R. K. Zeigler.

$5{\cdot}02 \times 10^{-4}$M, $[H^+] = 0{\cdot}01$M. Under these conditions the first stage is (initially) an order of magnitude faster than the second, and only after >90% do the rates become comparable. A two-stage reaction was observed with a plot of log (O.D.$_t$ − O.D.$_\infty$) against time for the second stage showing linearity up to 90—95% completion. At 25 °C, the value of k_4 averaged from 3 runs

TABLE 4

Kinetic data for the second stage of reaction,[a] monitored at $\lambda = 430$ nm, 35 °C, $I = 2{\cdot}0$M ($LiClO_4$). The figures in parentheses represent the numbers of runs averaged

$[H^+]$/M	$10^2[Cr^{2+}]$/M	$10^4[Co^{III}_2]$/M	k_4/s^{-1}
0·043	2·57	9·5	0·129 (3)
0·117	0·63	9·5	0·149 (3)
0·117	1·51	9·5	0·157 (3)
0·117	2·56	9·5	0·141 (3)
0·117	5·12	9·5	0·141 (2)
0·117	5·12	6·0	0·147 (1)
0·117	5·04	3·0	0·145 (3)
0·20	2·58	9·5	0·144 (3)
0·29	2·57	9·5	0·157 (3)
0·50	2·59	9·5	0·192 (3)

[a] k_4 Was evaluated after separation of two consecutive reactions.

was $5{\cdot}3 \times 10^{-2}$ s^{-1}, which is consistent with the higher value at 35°, $k_4 = 0{\cdot}123$ s^{-1}, $[H^+] = 0{\cdot}01$M. The difference in rate constant for a 10 °C increment of temperature suggests an enthalpy of activation of some 12—15 kcal mol^{-1}.

Third Stage of the Cr^{2+} *Reduction of the* μ*-Amido-*μ*-peroxo-complex.*—Kinetic data for the third stage were obtained under the same conditions as described above. Rate constants were evaluated from the latter part of the plots of log (O.D.$_t$ − O.D.$_\infty$) *versus* time, which were generally linear to at least 75% completion (see Figure 2). Rate constants k_5, at 35 °C, $I = 2{\cdot}0$M ($LiClO_4$), are once again independent of $[Cr^{2+}]$, for an 8-fold variation in reductant, and also independent of $[H^+]$ in the range

TABLE 5

Kinetic data for the third observable stage in the Cr^{2+} reduction of the μ-amido-μ-peroxo-complex (B). Reaction was monitored at $\lambda = 430$ nm, 35°, $I = 2{\cdot}0$M ($LiClO_4$). Figures in parentheses indicate the numbers of runs averaged

$[H^+]$/M	$10^2[Cr^{2+}]$/M	$10^4[Co^{III}_2]$/M	10^2k_5/s^{-1}
0·117	1·51	9·5	2·15 (3)
0·117	2·56	9·5	2·25 (2)
0·117	5·12	9·5	2·07 (2)
0·117	5·12	6·0	2·12 (1)
0·117	5·04	3·0	2·14 (2)
0·117	0·63	9·5	1·90 (2)
0·20	2·58	9·5	2·10 (3)
0·29	2·57	9·5	2·13 (3)
0·50	2·59	9·5	2·21 (3)

$[H^+] = 0{\cdot}117$ to 0·50M (see Table 5). The data in Table 5 support a rate law (7) where (D) is not necessarily

$$\frac{-\mathrm{d}}{\mathrm{d}t}[\mathrm{D}] = k_5[\mathrm{D}] \qquad (7)$$

the initial product of the second stage as will be discussed later. A least-squares treatment gives $k_5 = (2{\cdot}12 \pm 0{\cdot}08) \times 10^{-2}$ s^{-1} at 35 °C.

Final Stage of the Cr^{2+} *Reduction of the* μ*-Amido-*μ*-peroxo-complex.*—Absorbance decreases at $\lambda = 510$ nm were followed on a Unicam SP 500 spectrophotometer. This wavelength was chosen such that an optical density change ΔO.D. of *ca.* 0·2 units could be monitored. With $[Cr^{2+}]$ in 90- to 270-fold excess of initial dicobalt(III) concentration, plots of log (O.D.$_t$ − O.D.$_\infty$) *versus* time were linear to between 90% and 97% completion. Initial concentrations of Cr^{2+} were sufficiently high that there was no interference from earlier stages. At 35 °C reaction was first order in both reactants and for $[H^+]$ in the range 0·08—0·50M there was no dependence upon $[H^+]$ (see Table 6). Rate law (8) applies therefore where

$$\frac{\mathrm{d}}{\mathrm{d}t}[\mathrm{Product}] = k_6[Co^{III}_2][Cr^{2+}] \qquad (8)$$

a least-squares treatment gives $k_6 = (1{\cdot}09 \pm 0{\cdot}07) \times 10^{-3}$ l mol^{-1} s^{-1}.

TABLE 6

Kinetic data for the final stage Cr^{2+} reduction of the μ-peroxo-complex (B), monitored at $\lambda = 510$ nm, 35 °C, $I = 2{\cdot}0$M ($LiClO_4$)

$[H^+]$/M	$10^2[Cr^{2+}]$/M	$10^4[Co^{III}_2]$/M	10^3k_6/l mol^{-1} s^{-1}
0·08	2·5	3·0	1·10
0·14	5·0	1·5	1·16
0·14	4·7	5·0	1·01
0·14	8·1	3·0	1·09
0·14	5·0	3·0	1·01
0·14	2·5	3·0	1·12
0·25	2·5	3·0	1·06
0·50	2·5	3·0	1·19

Spectra of Reactants, Intermediates, and Products of Reduction.—Information regarding the spectra of intermediates formed during the Cr^{2+} reduction of (II) was obtained at 25 °C on a Unicam SP 800 (recording) spectrophotometer, between 700 and 350 nm. The spectrum of a solution of (II) present as (B) was first recorded to indicate the starting point of reaction (see Figure 3). Various solutions were then made up in which Cr^{2+} was added to (B) in 1 : 1, 2 : 1, and 3 : 1 ratios.

Run solutions at 25 °C, $I = 2{\cdot}0$M, $[Co^{III}_2] = 2{\cdot}5 \times 10^{-3}$M, $[H^+] = 0{\cdot}15$M, and $[Cr^{2+}]$ in the range 2·75 to $8{\cdot}25 \times 10^{-3}$M (5% excess of $[Cr^{2+}]$), were scanned between 350 and 700 nm and optical density readings converted into molar absorbance coefficients. The resulting spectra are displayed in Figure 4. Since the second observable stage upon reduction of the μ-peroxo-complex is independent of $[Cr^{2+}]$ the product of a 1 : 1 reaction observed in these experiments is most probably the product of this second stage. The spectrum of the product of the first stage was obtained using the stopped-flow apparatus. At 25 °C, $I = 2{\cdot}0$M, $[H^+] = 0{\cdot}1$M, $[Cr^{2+}] = 1{\cdot}03 \times 10^{-2}$M, and $[Co^{III}_2] = 4{\cdot}0 \times 10^{-4}$M the absorbance at the end of the first stage was measured from oscilloscope traces. The same run at wavelengths between 390 and 700 nm ($\Delta\lambda = 10$ nm) was monitored, and molar absorbance coefficients calculated from these optical density readings, after the stopped-flow path length l had been

estimated at 1·92 cm. The spectrum obtained is displayed in Figure 3.

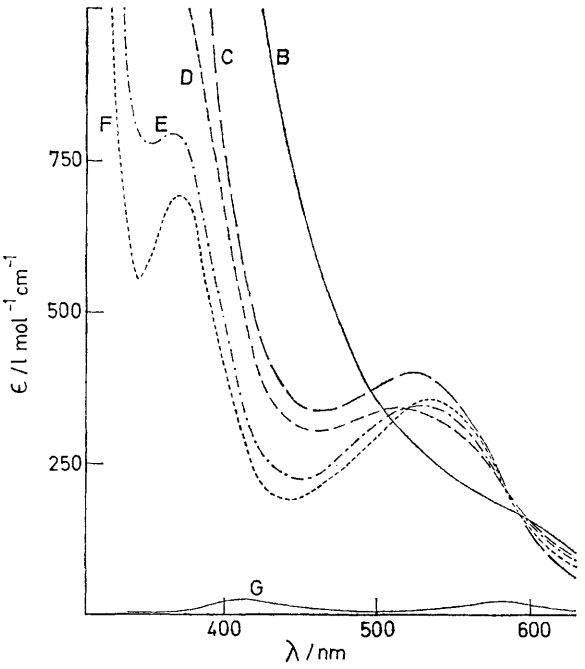

FIGURE 3 Spectra of the μ-amido-μ-peroxo-complex (B) and of intermediates obtained on reduction of (B) with Cr^{2+}. Spectrum C refers to the 1 : 1 reaction product before isomerisation, and spectrum D to the product after isomerisation. Spectrum E is obtained for a 2 : 1 [Cr^{2+} : (B)] reaction), F for a 3 : 1 reaction, and G (final product) for a 4 : 1 reaction. All spectra were measured at 25 °C, I = 2·0M ($LiClO_4$)

The first three observable stages are complete within 10 min and in the case of 1 : 1, 2 : 1, and 3 : 1 products the spectra were recorded after calculating the amount of time required to give the relevant product.

The spectrum of the final product of the reaction is not as readily obtained, since a second-order rate constant for $k_6 = 1{\cdot}1 \times 10^{-3}$ l mol^{-1} s^{-1} requires a period of days for completion with $[Cr^{2+}] = 5 \times 10^{-4}$M. An unambiguous assignment as to whether mononuclear or binuclear chromium(III) products are formed is not possible, but the cobalt(III) chromophore which clearly dominates the visible spectrum up to the final stage of reduction is no longer present. A run with initial $[Cr^{2+}] = 2{\cdot}1 \times 10^{-3}$M, $[Co^{III}{}_2] = 5 \times 10^{-4}$M, I = 2·0M, and $[H^+]$ = 0·1M was heated and maintained at 50 °C for 4 days. The resulting spectrum indicated a chromium(III) species present, $\lambda_{max.}$ 412 and 578 nm, but doubt remains as to whether this represents the primary product of the final stage.

Ion-exchange Separation of Products.—All reactions were carried out at 25 °C, I = 2·0M, with $[Co^{III}{}_2]$ in the range 1·32 to 6·5 × 10^{-3}M. Solutions of chromium(II) were syringed into previously deoxygenated solutions of oxidant to give ratios of $[Cr^{2+}]/[Co^{III}{}_2]$ in the range 1·05 to 4·1, as required. These solutions were given sufficient time for reaction and then transferred onto a column of Dowex 50W-X12 ion-exchange resin. Hexaaquochromium(III) was eluted using 1·0M-$HClO_4$ and determined by oxidation to CrO_4^{2-} using H_2O_2 in 1·0M-NaOH. A variety of related oxidants were investigated and the results of these experiments are given in Table 7. All chromium(III) products are quoted relative to dicobalt(III) reactants, and the effect of $[H^+]$ upon products was investigated in several cases.

Although most of these reactions were straightforward, particular attention to the practical details is necessary in several cases. First, when a 4 : 1 ratio of Cr^{2+} to μ-peroxo-complex was taken, entry 6 in Table 7, the complete reaction was very slow and required around 4 days at 50 °C. A control experiment with the chromium(III) dimer $(H_2O)_4Cr(OH)_2Cr(H_2O)_4^{4+}$ [9] showed that there was some decomposition over this time period, consequently a dimeric chromium(III) primary product cannot be entirely excluded.

Reduction of the related singly bridged μ-superoxo-complex (III) by Cr^{2+} (1 : 1 reaction) gives approximately 25% of the total product as Cr^{3+}.[4] A further investigation was carried out by measuring not only the yield of Cr^{3+} as primary product but also the amount of μ-superoxo-complex consumed. With $[Cr^{2+}] = 5 \times 10^{-3}$M, $[Co^{III}{}_2] = 5 \times 10^{-3}$M, spectrophotometric measurement of the products at λ = 670 nm indicated 26·4% consumption of the μ-superoxo-complex in good agreement with the experimentally determined 24·5% production of Cr^{3+} (see Table 7). It can be concluded that in this case decomposition of the μ-peroxo-complex to give Co^{2+} and O_2 is more rapid than Cr^{2+} reduction.

TABLE 7

A summary of ion-exchange results for the Cr^{2+} reduction of related μ-superoxo- and μ-peroxo-dicobalt(III) complexes at 25 °C, I = 2·0M ($LiClO_4$). Figures in parentheses indicate the numbers of runs averaged

Oxidant	Equivalents of [a] Cr^{2+} added	Equivalents of [a] Cr^{3+} produced
$\mu(NH_2,O_2^-)$ (I)	1·03	0·97 (3)
	2·05	1·05 (1)
$\mu(NH_2,O_2^{2-})$ (II)	1·03	0·08 (1)
	2·05	0·98 [b] (3)
	3·05	1·65 [b] (3)
	4·10	2·6 (2)
$\mu(O_2^-)$ (III)	1·03	0·96 [c] (2)

[a] Cr^{2+} reactant and Cr^{3+} product measured relative to the number of moles of dicobalt(III) complex initially present. Allowance for Cr^{3+} initially present in Cr^{2+} reaction solutions has been made in column 3. [b] Hydrogen-ion concentration varied between 0·1 and 0·8M; the product distribution was unaffected. [c] The value in column 3 is based upon the amount of μ-superoxo-complex consumed.

Chromium(II) *Reduction of μ-Amido-μ-hydroperoxo-bis-[bis(ethylenediamine)cobalt*(III)].—Absorbance changes at λ = 500 nm were monitored using stopped-flow apparatus. At 25 °C, I = 2·0M ($HClO_4$), $[Co^{III}{}_2]_{total} = 6{\cdot}25 \times 10^{-4}$M, and $[Cr^{2+}] = 5{\cdot}45 \times 10^{-3}$M the concentration of the hydroperoxo-complex [AH] is esti-

[9] G. Thompson, Ph.D. Thesis, University of California, Berkeley, 1964, microfilm, UCRC 11410.

mated to be *ca.* 50% using K_1 and K_2 for the (B)/(BH) and (AH)/(BH) equilibria at $I = 0{\cdot}245$M ($NaClO_4$).[7] At $\lambda = 500$ nm both (B) and (BH) have similar absorbance coefficients (ε *ca.* 350 l mol^{-1} cm^{-1}),[7] as also do the intermediate products of reduction of a (B)/(BH) mixture ($\varepsilon = 370$ l mol^{-1} cm^{-1}) (see Figure 3). The reasonable assumption that inner-sphere Cr^{2+} reduction of (AH) results in a species similar to that produced from the second stage observed during the Cr^{2+} reduction of the μ-peroxo-complex (see Discussion) means that an increase in absorbance due to a reaction of (AH) with Cr^{2+} will result at $\lambda = 500$ nm.

Very small absorbance changes were observed and the initial and final optical densities correspond to (AH) contributing both before and after reaction. Unless the Cr^{2+} reduction of (AH) at $\lambda = 500$ nm produces negligible absorbance change it must be concluded that on the scale of stopped-flow reaction-time bases (AH) does react. The (B) and (BH) species will, of course, react with Cr^{2+} but will not result in any absorbance change; (AH) will subsequently isomerise to the (B)/(BH) mixture as described by Mori and Weil ($k = 0{\cdot}11$ s^{-1} at 25 °C for formation of an equilibrium mixture).[7] Assuming a first-order dependence upon $[Cr^{2+}]$ a limiting rate of $\leqslant 0{\cdot}1$ l mol^{-1} s^{-1} is suggested for the Cr^{2+} reduction of (AH).

Vanadium(II) *Reduction of the μ-Amido-μ-superoxo-complex.*—The reaction was monitored at $\lambda = 687$ nm, a peak position for the μ-superoxo-complex ($\varepsilon = 485$ l mol^{-1} cm^{-1}), using a stopped-flow spectrophotometer. At 25 °C, $I = 2{\cdot}0$M ($LiClO_4$), $[H^+] = 0{\cdot}1$M, $[Co^{III}_2] = 5{\cdot}0 \times 10^{-4}$M, and $[V^{2+}] = 5{\cdot}1 \times 10^{-3}$M it was not possible to observe any rate process. The final absorbance reading (monitored within the 5 ms required for mixing on the stopped-flow apparatus) corresponded to complete consumption of the μ-superoxo-complex. It was concluded that the reaction under these conditions is too fast to follow assuming a first-order dependence upon $[V^{2+}]$; a lower limit for the reduction is $2{\cdot}5 \times 10^5$ l mol^{-1} s^{-1}.

Vanadium(II) *Reduction of the μ-Amido-μ-peroxo-complex.*—Using the stopped-flow apparatus absorbance changes were monitored at $\lambda = 450$ nm, with $[V^{2+}]$ in 25- to 75-fold excess of $[Co^{III}_2]$. Initial Co^{III}_2 solutions contained no acid, thus ensuring only (B) and (BH) present if reduction by V^{2+} is fast. Plots of log (O.D.$_t$ − O.D.$_\infty$) *versus* time were only linear for the latter half of reaction and it was concluded that there were two stages of reaction. First-order rate constants for both stages were obtained after applying the consecutive-reaction treatment, and are listed in Table 8, k_7 and k_8 respectively.

The first stage rate constant k_7 appears to be independent of $[V^{2+}]$ and $[H^+]$ over a 3 to 4 fold variation of both (Table 8), and consequently is attributed to an isomerisation of (BH) ⟶ (AH) [7] which is initiated after hydrogen ions are introduced along with the V^{2+} solution upon mixing. The rate constant $k_7 = 0{\cdot}127 \pm 0{\cdot}015$ s^{-1} at 25 °C is in good agreement with the value found at $I = 0{\cdot}245$M ($NaClO_4$), $k = 0{\cdot}112$ s^{-1} at 25 °C.[7] The reaction of (B) with V^{2+} is slower than isomerisation (BH) ⟶ (AH).

The second stage is first order in $[V^{2+}]$ and $[Co^{III}_2]$ and has a somewhat complex acid dependence. If all the species (B), (BH), and (AH) are considered as

TABLE 8

Kinetic data for the V^{2+} reduction of the μ-amido-μ-peroxo-complex at 25 °C, $\lambda = 450$ nm, $I = 2{\cdot}0$M ($LiClO_4$). Figures in parentheses indicate the number of runs averaged for the last two columns

$[H^+]$ / M	$10^3[V^{2+}]$ / M	$10^4[Co^{III}_2]$ / M	k_7 [a] / s^{-1}	$k_8/[V^{2+}]$ / l mol^{-1} s^{-1}
0·25	9·65	4·0	0·129	1·05 (2)
0·50	9·65	4·0	0·130	0·82 (3)
0·50	30·1	4·0	0·110	0·81 (2)
0·97	9·95	4·0	0·140	0·65 (2)

[a] k_7 Obtained as the first stage of two reactions separated using the consecutive reaction treatment.

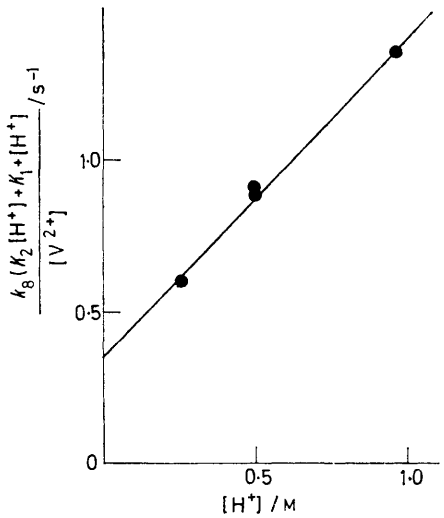

FIGURE 4 The V^{2+} reduction of the μ-amido-μ-peroxo-complex with (B), (BH), and (AH) present at 25 °C, $I = 2{\cdot}0$M ($LiClO_4$). The ordinate is taken on the left-hand side of equation (11). The pseudo-first-order rate constant k_8 corresponds to the second of two consecutive reactions monitored at 450 nm

possible reactants a rate law (9) results, and upon expressing the individual components (B), (BH), and (AH) in

$$\frac{-\mathrm{d}}{\mathrm{d}t}[C_0] = V^{2+}(k_B[B] + k_{BH}[BH] + k_{AH}[AH]) \quad (9)$$

terms of total dicobalt(III) concentration C_0, equation (9) may be rewritten as (10). This may be expressed in

$$\frac{-\mathrm{d}}{\mathrm{d}t}C_0 = \frac{[V^{2+}]C_0(k_BK_1 + k_{BH}[H^+] + k_{AH}K_2[H^+])}{K_2[H^+] + K_1 + [H^+]} \quad (10)$$

terms of the observed rate constant k_8, as in equation (11).

$$\frac{k_8}{[V^{2+}]}(K_2[H^+] + K_1 + [H^+]) = k_BK_1 + k_{BH}[H^+] + k_{AH}K_2[H^+] \quad (11)$$

A plot of the left-hand side of (11) against $[H^+]$ (see Figure 4), yields k_BK_1 as intercept and a composite

gradient of $(k_{BH} + k_{AH}K_2)$. At 25 °C $I = 2{\cdot}0$M, a value of $K_1 = 0{\cdot}046$M (Table 3) gives $k_B = 7{\cdot}7 \pm 1$ l mol^{-1} s^{-1}. The composite rate constant for either one or both of (BH) and (AH) reacting is 1·04 l mol^{-1} s^{-1} (slope of Figure 4). If both (BH) and (AH) are reactants, and $K_2 = 1{\cdot}11$ (independent of ionic strength) at 25° C,[7] then k_{AH} and k_{BH} are <1 l mol^{-1} s^{-1}, but if only one species is a reactant $k \sim 1$ l mol^{-1} s^{-1}. On the basis of the rate law it is not possible to distinguish between (BH) and (AH) as reactants.

DISCUSSION

Reduction of the μ-amido-μ-peroxo-complex (II) is considered first. This occurs by a stepwise series of reactions, not all of which are reduction processes. On the basis of ion-exchange experiments, spectra, and kinetic data, it has been possible to partially separate the various stages.

The first stage of the Cr^{2+} reduction of the μ-amido-μ-peroxo-complex [(B) form] is fast, $k_2 = 2100 \pm 60$ l mol^{-1} s^{-1} at 25 °C (Table 3). Complete retention of chromium(III) with the formation of a cobalt(III)–chromium(III) binuclear species is inferred since no Cr^{3+} is liberated into solution. Moreover the spectrum of this intermediate, measured using the stopped-flow apparatus, clearly indicates the presence of a cobalt(III) chromophore. Inner-sphere reduction of (B) may occur at either oxygen of the peroxo-bridge, and unless electron transfer through two oxygen centres rather than one is preferable, the product of reaction will be predominantly a species (C) as indicated in reaction (12).

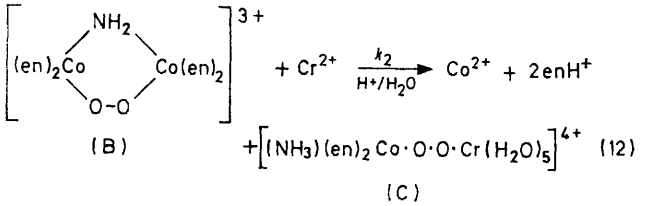

(B) (C) (12)

Contributions from the parallel reduction of the protonated species (BH) most probably result in the production of (C) also. However, these are relatively small so that it cannot be certain that this path is effective. An estimate for k_3 taken from computed results gives $k_3 = 16 \pm 6$ l mol^{-1} s^{-1} at 25 °C, which corresponds to 0·8% of the reactivity on protonation of (B). Reduction of the isomeric hydroperoxo-complex (AH) on the basis of absorbance data is considerably slower than Cr^{2+} reduction of (B) and (BH). An upper limit of 0·1 l mol^{-1} s^{-1} for the reduction rate constant suggests that attack *via* the pendant oxygen is again effectively blocked upon protonation. Available evidence for reactions of the hydroperoxo-complex with chloride,[6] bromide,[6] and iodide [10] suggests moreover that (AH) probably undergoes two-electron transfer more readily than one-electron transfer. This incompatibility between the one-electron donor, Cr^{2+}, and the two-electron acceptor (AH) is expected to lower considerably the rate constant for electron transfer. An acid dissociation constant $K_a = 10^{-11}$ mol l^{-1} [7] rules out attack *via* the deprotonated hydroperoxo-complex under the conditions investigated.

The second and third observable stages of reaction, giving first (D) and then (E) are independent of Cr^{2+} and some form of isomerisation or decay process is required. For the second stage the product of reaction has a spectrum not too dissimilar from that of (C) suggesting that a mixed binuclear species is still present. A spectrophotometric shift to shorter wavelength in going from (C) to the product of the second stage, (D), is apparent (Figure 3), as was found for the transformation (B) ⟶ (AH).[7] Although no activation parameters are available the observed rates resemble those for the isomerisation (BH) ⟶ (AH) reported by Mori and Weil,[7] and an isomerisation reaction is proposed here, equation (13). Reaction (13) is observed even when a

$$\underset{(C)}{[(NH_3)(en)_2Co{\cdot}O{\cdot}O{\cdot}Cr(H_2O)_5]^{4+}} \xrightarrow[k_4]{H^+} \underset{(D)}{[(NH_3)(en)_2Co(OH){\cdot}O{\cdot}Cr(H_2O)_5]^{5+}} \quad (13)$$

1 : 1 ratio of $[Cr^{2+}]$ to $[Co^{III}{}_2]$ is taken, which requires (C) as the product of the first stage of reduction.

Inspection of the product spectrum after 3 equivalents of Cr^{2+} have been consumed by 1 equivalent of the μ-amido-μ-peroxo-complex (B) shows that a cobalt(III) chromophore still dominates the spectrum (see Figure 3). Product analysis after a 3 : 1 reaction indicates that 1 equivalent of chromium(III) is still present in a mixed binuclear species (see Table 7). Since a mixed binuclear species is already present after a 1 : 1 reaction, the further consumption of 2 equivalents of Cr^{2+} must involve reduction of the peroxo-bridge.

Although the second stage may be reasonably described by equation (13) a precise interpretation of data for subsequent reduction of the peroxo-bridge is not possible. Product analysis confirms that reduction by Cr^{2+} is occurring, but kinetic data demand that Cr^{2+} attack is non-rate-determining, since no dependence upon $[Cr^{2+}]$ is observed during the course of the second and third stages. It is, therefore, not possible to state categorically the stage (or stages) at which Cr^{2+} reduction occurs.

Several reaction schemes, with isomerisation (or decomposition) and Cr^{2+} reduction incident at different stages, may explain the observations subsequent to the formation of (D); these are as follows. (*a*) Rapid reduction of (D) by two equivalents or Cr^{2+}, producing an O_2^{4-} bridging ligand [equation (14)]. The observed third stage would then correspond to oxygen-oxygen scission within this resultant species [equation (15)].

[10] R. Davies, M. B. Stevenson, and A. G. Sykes, *J. Chem. Soc.* (*A*), 1970, 1261.

$$[(NH_3)(en)_2Co(OH)Cr(H_2O)_5]^{5+} + 2Cr^{2+} \longrightarrow [(NH_3)(en)_2Co(OH)Cr(H_2O)_5]^{3+} + 2Cr^{3+} \quad (14)$$

$$[(NH_3)(en)_2Co(OH)Cr(H_2O)_5]^{3+} \xrightarrow{H^+} [(NH_3)(en)_2Co{\cdot}OH{\cdot}Cr(H_2O)_5]^{5+} + H_2O \quad (15)$$

(*b*) A second isomerisation of (D) [equation (16)], representing the third observed stage, followed by fast reduction of the peroxo-bridge by two equivalents of Cr^{2+} [equation (17)].

$$[(NH_3)(en)_2Co(OH)Cr(H_2O)_5]^{5+} \longrightarrow [(NH_3)(en)_2Co(O_2)Cr(H_2O)_5]^{4+} \quad (16)$$

$$[(NH_3)(en)_2Co(O_2)Cr(H_2O)_5]^{4+} + 2Cr^{2+} \xrightarrow{H^+} [(NH_3)(en)_2Co{\cdot}OH{\cdot}Cr(H_2O)_5]^{5+} + 2Cr^{3+} + H_2O \quad (17)$$

(*c*) Fast one-equivalent Cr^{2+} reduction of the peroxo-bridge in (D), by an inner-sphere mechanism [equation (18)], to give an O_2^{3-} bridge. Rate-determining scission

$$[(NH_3)(en)_2Co(OH)Cr(H_2O)_5]^{5+} + Cr^{2+} \longrightarrow [(NH_3)(en)_2Co(O_2)Cr(H_2O)_5]^{7+} \quad (18)$$
(Cr–OH)

of the oxygen–oxygen bond would then provide the third observed stage, (19), and rapid Cr^{2+} reduction of the mononuclear product of (19) completes reduction of the peroxo-bridge, (20).

$$[(NH_3)(en)_2Co(OH)Cr(H_2O)_5]^{7+} \longrightarrow [(NH_3)(en)_2Co{\cdot}OH{\cdot}Cr(H_2O)_5]^{5+} + CrO^{2+} \quad (19)$$
(Cr–OH)

$$Cr^{2+} + CrO^{2+} \longrightarrow (Cr^{III})_2 \quad (20)$$

(*d*) Fast one-equivalent Cr^{2+} reduction of the peroxo-bridge by an outer-sphere mechanism to give an O_2^{3-} bridge, (21), which subsequently undergoes rate-determining decomposition with the formation of a radical

$$[(NH_3)(en)_2Co(OH)Cr(H_2O)_5]^{5+} + Cr^{2+} \longrightarrow [(NH_3)(en)_2Co(O_2)Cr(H_2O)_5]^{4+} + Cr^{3+} \quad (21)$$

species (possibly OH), (22). The radical then reacts rapidly with a second Cr^{2+}. These various alternatives, particularly (*a*)—(*c*), have certain inadequacies which are now considered.

$$[(NH_3)(en)_2Co(OH)Cr(H_2O)_5]^{4+} \xrightarrow{H^+} [(NH_3)(en)_2Co{\cdot}OH{\cdot}Cr(H_2O)_5]^{5+} + OH \quad (22)$$

Scheme (*a*) may be ruled out for two reasons. First, chromium(II) reduction of the μ-hydroperoxo-complex (AH) is slow, k_{AH} (25 °C) $\leqslant 0{\cdot}1$ l mol^{-1} s^{-1}. Reduction of the related μ-hydroperoxo-complex (D) is expected to be even slower, since a chromium(III) centre now replaces the cobalt(III) centre in (AH). Consequently, a fast reduction of (D) by 2 equivalents of Cr^{2+} is considered highly improbable. Secondly, the product of a two equivalent reduction is the O_2^{4-} bridging group. The bond order of such a species is zero and oxygen–oxygen scission should effectively be spontaneous. The observed third stage, k_5 (35 °C) $= 2{\cdot}1 \times 10^{-2}$ s^{-1}, is far too slow for such a process.

Scheme (*b*) is considered improbable because a second isomerisation step occurs prior to Cr^{2+} reduction, and yet another isomeric form of the cobalt(III)–chromium(III) μ-peroxo-complex is required.

Scheme (*c*) is unlikely again because Cr^{2+} reduction of the hydroperoxo-bridge is unlikely to be rapid. Equation (20) would be expected to give substantial amounts of binuclear chromium(III) product.

The remaining possibility, scheme (*d*), fits the experimental observations far more closely than (*a*)—(*c*). A rapid outer-sphere Cr^{2+} reduction of (D) is required however. Assuming a first-order dependence upon Cr^{2+} for reaction (21), and that the first-order rate constant for (21) is at least 3-fold faster than the preceding second stage of reaction, the second-order rate constant for (21) must be at least 10^2 l mol^{-1} s^{-1} at 35 °C. This value is more than 3 orders of magnitude larger than that for Cr^{2+} reduction of (AH) ($k_{AH} \leqslant 0{\cdot}1$ l mol^{-1} s^{-1}), and such a discrepancy is difficult to reconcile unless loss of a proton from the hydroperoxo-bridge is more extensive or the bonding is different to that of known hydroperoxo-complexes, *e.g.* (AH), and is possibly similar to that indicated for the product of (16). The product of (21) has an O_2^{3-} bridging group, for which a bond order of 0·5 is appropriate. The O_2^{3-} bridge is presumably unstable and rate-determining scission of the oxygen–oxygen bond is predicted. The rate constant $k_5 = 0{\cdot}021$ s^{-1} at 25 °C could well be consistent with this mechanism.

Up to this stage the product spectrum has always shown evidence of a cobalt(III) chromophore, and it is only during the final stage of reduction that it disappears (see Figure 3). Reduction is slow, $k_6 = (1{\cdot}09 \pm 0{\cdot}10) \times 10^{-3}$ l mol^{-1} s^{-1} at 35 °C, which is characteristic of an outer-sphere mechanism. This is consistent with reaction (23). Although the product analysis was

$$[(NH_3)(en)_2Co(OH)Cr(H_2O)_5]^{5+} + Cr^{2+} \xrightarrow{H^+/H_2O} 2Cr^{3+} + Co^{2+} + 2enH^+ + NH_4^+ \quad (23)$$

difficult, the results of ion-exchange experiments and spectra tend to support predominantly Cr^{3+} as the primary product of the final stage, as in (23). If a mononuclear cobalt(III) product was present prior to the final stage this would presumably have to be $[Co(en)_2(NH_3)(H_2O)]^{3+}$ which reacts rapidly with Cr^{2+}.

The multi-step Cr^{2+} reduction of the μ-amido-μ-peroxo-complex is somewhat complicated and it is perhaps only certain that the first and final stages of reduction are as presented. A scheme for the intermediate stages has been suggested and although based upon what is believed to be sound indirect argument it is somewhat speculative in nature. For this reason the intermediate steps will not be discussed further.

Unequivocal evidence for the inner-sphere reduction of (B) has been presented and this is also supported by data from the V^{2+} reduction. Although no activation parameters are available, k_B (25 °C) for V^{2+} reduction of (B) falls within the range for V^{2+} substitution-controlled inner-sphere reductions, $k_B = 7{\cdot}7 \pm 1$ l mol^{-1} s^{-1}. It is uncertain whether the $[H^+]$-dependent second term in (11) is due to reaction of (BH) and/or (AH) with V^{2+}. The upper limit for rate constants for the reduction of BH and/or AH are at the lower end of the V^{2+} substitution controlled range. Without knowing activation parameters a firm assignment is not possible, and at this juncture outer-sphere processes cannot be ruled out, and indeed may be more likely since the peroxo-group in (BH) and (AH) is protonated.

The product from the Cr^{2+} reduction of (B) provides the first example of a complex containing a μ-peroxo-bridge with two different metal ions. Similarly, reactions of (B) with nitric oxide,[11] nitrous acid,[12] and sulphite [12] also proceed with inner-sphere (or bonded) attack of the reductant. The products obtained indicate inner-sphere attack at the peroxo-bridge and the μ-amido-μ-nitrito- and μ-amido-μ-sulphato-complexes result.

Reduction of the μ-superoxo-complex (I) by both Cr^{2+} and V^{2+} is too fast to follow using the stopped-flow technique. Rate constants in excess of $1{\cdot}4 \times 10^5$ and $2{\cdot}5 \times 10^5$ l mol^{-1} s^{-1} are required for Cr^{2+} and V^{2+} respectively, and although these do not limit the Cr^{2+} reduction, the rate constant for V^{2+} is far in excess of the inner-sphere substitution-controlled limit. Reduction of the μ-superoxo-complex (I) by V^{2+} is outer-sphere.

Although the rate constant for Cr^{2+} reduction does not necessarily exceed the rate constant for water substitution the available information supports an outer-sphere reduction mechanism. First, the product of reactions with Cr^{2+} and (I) in 1 : 1 ratios gave 96% $Cr(H_2O)_6^{3+}$ and μ-amido-μ-peroxo-complex, indicating outer-sphere reduction. Secondly, the interactions between reactants of the same charge will produce an unfavourable outer-sphere ion-pair. The basis of these calculations has been outlined previously, and although the calculations are necessarily approximate they have the virtue of providing realistic corrections to observed activation parameters.[13]

With binuclear cobalt(III) complexes the ion-pair association constant is very sensitive to the closeness of approach of ions in the ion-pair complex. The method is illustrated by considering ion-pair formation between the μ-superoxo-complex (I) and Cr^{2+} at 5 Å separation, $I = 1{\cdot}0$M ($LiClO_4$). At 25 °C, for a charge product of +8 an association constant $K_0 = 10^{-2{\cdot}6}$ l mol^{-1} is calculated. The observed rate of reduction k_1 is the product of a fast ion-pair formation constant (K_0) and electron-transfer rate constant (k), such that $k_1 = kK_0$, and with $K_0 = 10^{-2{\cdot}6}$ l mol^{-1}, $k_1 \geqslant 1{\cdot}4 \times 10^5$ l mol^{-1} s^{-1}, a value for $k \geqslant 5{\cdot}6 \times 10^7$ s^{-1} results. This value for k borders on the substitution-controlled limit for Cr^{2+} reactions (10^8 to 10^9 s^{-1}),[14] and reduction may be outer sphere for this reason alone.

In support of the outer-sphere assignment of mechanism for Cr^{2+} reduction of (I) there is much evidence suggesting outer-sphere reduction of several related superoxo-bridged dicobalt(III) complexes by a variety of reductants. Hoffman and Taube [4] have studied the reduction of the singly bridged μ-superoxo-complex (III), by Cr^{2+}, V^{2+}, and Eu^{2+}, and the Fe^{2+} reduction has also been studied.[5] The ratio $k_{Cr}/k_V = 0{\cdot}024$ is consistent with outer-sphere Cr^{2+} and V^{2+} reductions. A linear free-energy relationship is observed for one-equivalent oxidations by the μ-superoxo-complex (II) and hexaaquoiron(III) (acid-independent pathway) respectively by the above series of reductants.[15] This clearly indicates an outer-sphere mechanism for the reaction of Fe^{2+} with (III). A satisfactory linear free-energy relationship is also observed for the reduction of a series of μ-superoxo-dicobalt(III) complexes by Fe^{2+} and the μ-peroxo-complex (B) [16] [see Figure 5 and equation (24)],

$$\log k_{Fe}^{II} = (1{\cdot}14 \pm 0{\cdot}08) \log k_P - (0{\cdot}1 \pm 0{\cdot}1) \quad (24)$$

and in view of the assignment made for the reaction of (III) with Fe^{2+} is indicative of outer-sphere reduction in all cases. With the μ-peroxo-reductant the reaction is independent of $[H^+]$ and each superoxo-complex is reduced to the corresponding peroxo-complex.

Reductions of the μ-superoxo-complex (I) by NO,[11] NO_2^-,[12] and SO_3^{2-} [12] are all demonstrably outer sphere, and it is once again concluded that reaction is occurring *via* a non-bonded activated complex. At present there are no known examples for inner-sphere reaction of (I). All the available evidence points to outer-sphere reduction for a variety of μ-superoxo-dicobalt(III) complexes. In certain cases an outer-sphere mechanism is called for simply because the electron-transfer rate is faster than substitution at the more labile reactant centre.[13] How-

[11] C. H. Yang, D. P. Keeton, and A. G. Sykes, *J.C.S. Dalton*, 1974, 1089.
[12] J. D. Edwards, C. H. Yang, and A. G. Sykes, *J.C.S. Dalton*, 1974, following paper.
[13] M. R. Hyde and A. G. Sykes, *J.C.S. Chem. Comm.*, 1972, 1340.
[14] T. J. Swift and R. E. Connick, *J. Chem. Phys.*, 1962, **37**, 307.
[15] M. R. Hyde, Ph.D. Thesis, University of Leeds, 1973.
[16] R. Davies, M. Mori, A. G. Sykes, and J. A. Weil, *Inorg. Synth.*, 1970, **12**, 197.

ever, there are also examples where this is not necessarily true and an alternative explanation is called for.

There is no evidence for protonation of the superoxo-bridge, whereas the peroxo-bridge in (II) readily protonates, $K_p = 7{\cdot}14$ l mol^{-1} at 25 °C, $I = 0{\cdot}0245$M.[7] The μ-peroxo-complex (II) has a great tendency for reaction by an inner-sphere path and the different mechanisms observed for (I) and (II) are consistent with non-donor and donor properties exhibited by the superoxo- and peroxo-bridges in these complexes. Chance degeneracy of the energy levels for the d_{xz} cobalt(III) orbital and the π_g^* orbital of O_2^- has been suggested [7] to explain the stability of the cobalt-superoxo-system. The degeneracy in such an extended molecular orbital

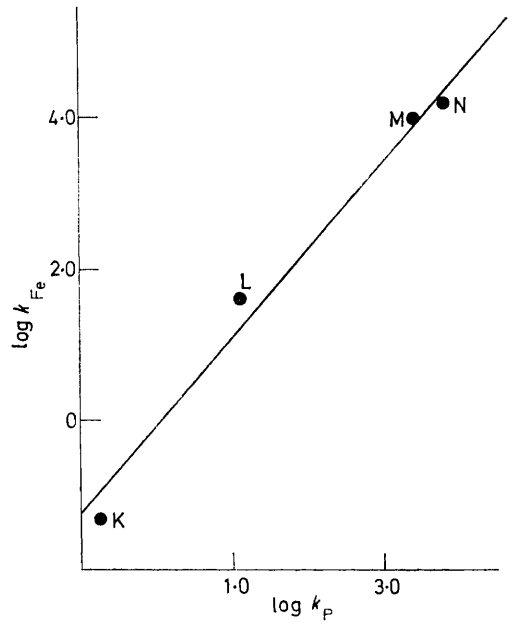

FIGURE 5 The log–log correlation of rate constants for the reductions of four μ-superoxo-complexes $(NH_3)_5Co{\cdot}O_2{\cdot}Co(NH_3)_5^{5+}$ K, $[(NH_3)_4Co{\cdot}\mu(NH_2,O_2){\cdot}Co(NH_3)_4]^{4+}$ L, $[(bipy)_2Co{\cdot}\mu(NH_2,O_2){\cdot}Co(bipy)_2]^{4+}$ M, and $[(phen)_2Co{\cdot}\mu(NH_2,O_2){\cdot}Co(NH_3)_4]^{4+}$ N with Fe^{2+} (k_{Fe}) and the μ-peroxo-complex $[(en)_2Co{\cdot}\mu(NH_2,O_2){\cdot}Co(en)_2]^{3+}$ (k_p). Data taken from reference 17

may well be the reason why the superoxo-bridge is a very poor donor group.

In the case of outer-sphere electron transfer a major contribution to the overall activation free energy comes from reorganisation of the inner co-ordination spheres of reactants. Although reduction by Cr^{2+} always requires a large reorganisation energy in going to the activated complex, the reorganisation term relevant to the oxidant will vary with each oxidant. Reduction of (I) by an outer-sphere mechanism gives (II), and the contribution from the dicobalt(III) complex to the structure of the activated complex must lie somewhere between (I) and (II). The geometries of (I) and (II) are quite similar and inner-co-ordination-sphere reorganisation is probably very small. The favourable geometries of (I) and (II) presumably enhance outer-sphere electron transfer to (I).

Summary.—The reaction scheme proposed for the five-equivalent reduction of μ-amido-μ-superoxo-bis[bis-(ethylenediamine)cobalt(III)] complex is somewhat complicated, and a brief synopsis of the observed rate processes at $I = 2{\cdot}0$M ($LiClO_4$) is included to clarify the situation.

(1) *Reduction of μ-amido-μ-superoxo-complex.* The reaction is too fast to follow using the stopped-flow apparatus and a lower limit for reduction has been estimated at

$$[(en)_2Co{\cdot}\mu(NH_2,O_2){\cdot}Co(en)_2]^{4+} + Cr^{2+} \longrightarrow [(en)_2Co{\cdot}\mu(NH_2,O_2){\cdot}Co(en)_2]^{3+} + Cr(H_2O)_6^{3+}$$

$1{\cdot}4 \times 10^5$ l mol^{-1} s^{-1} in the range 4—35 °C. Ion-exchange and spectrophotometric data indicate an outer-sphere mechanism for reduction.

(2) *First-stage reduction of μ-amido-μ-peroxo-complex.* The dominant pathway for Cr^{2+} reduction of the μ-peroxo-complex involves the deprotonated form. At

$$[(en)_2Co{\cdot}\mu(NH_2,O_2){\cdot}Co(en)_2]^{3+} + Cr^{2+} \xrightarrow{H^+/H_2O} [(NH_3)(en)_2Co{\cdot}O{\cdot}O{\cdot}Cr(H_2O)_5]^{4+} + Co^{2+} + 2enH^+$$

25 °C $k = 2100$ l mol^{-1} s^{-1}, $\Delta H^\ddagger = 7{\cdot}75 \pm 0{\cdot}25$ kcal mol^{-1}, $\Delta S^\ddagger = -17{\cdot}5 \pm 0{\cdot}9$ cal K^{-1} mol^{-1}. There was no evidence for formation of $Cr(H_2O)_6^{3+}$ and an inner-sphere reduction is proposed. Although the cobalt(III) product was not isolated its spectrum was obtained, and represents the first example of a complex containing a peroxo-ligand bridging two different metal ions.

(3) *Second-stage reduction μ-amido-μ-peroxo-complex.* Reaction is believed to involve isomerisation of the first-stage product and at 35 °C, $k = 0{\cdot}12 \pm 0{\cdot}14$ [H$^+$] s^{-1}.

$$[(NH_3)(en)_2Co{\cdot}O{\cdot}O{\cdot}Cr(H_2O)_5]^{4+} \xrightarrow{H^+} [(NH_3)(en)_2Co{\cdot}\underset{\displaystyle OH}{\underset{|}{O}}{\cdot}Cr(H_2O)_5]^{5+}$$

(4) *Third-stage reduction of μ-amido-μ-peroxo-complex.* Reduction of the peroxo-bridging ligand occurs between the observed second and final stages of reaction. There is no evidence for rate-determining Cr^{2+} attack and the reaction scheme becomes much more speculative. The scheme which best satisfies the experimental observations requires rapid reduction of the second-stage product, $k \geqslant 10^2$ l mol^{-1} s^{-1} at 35 °C.

$$[(NH_3)(en)_2Co{\cdot}\underset{\displaystyle OH}{\underset{|}{O}}{\cdot}Cr(H_2O)_5]^{5+} + Cr^{2+} \longrightarrow [(NH_3)(en)_2Co{\cdot}\underset{\displaystyle OH}{\underset{|}{O}}{\cdot}Cr(H_2O)_5]^{4+} + Cr^{3+}$$

Subsequent slow rate-determining scission of the oxygen–oxygen bond represents the observed third stage, $k_5 = 2{\cdot}1 \times 10^{-2}$ s^{-1} at 35 °C. Finally, reduction

$$[(NH_3)(en)_2Co{\cdot}\underset{\displaystyle OH}{\underset{|}{O}}{\cdot}Cr(H_2O)_5]^{4+} \xrightarrow{H^+} [(NH_3)(en)_2Co{\cdot}OH{\cdot}Cr(H_2O)_5]^{5+} + OH$$

of the OH radical by Cr^{2+} is non-rate-determining, and a rate constant in excess of 3 l mol^{-1} s^{-1} is required to account for the observations.

(5) *Final-stage reduction of μ-amido-μ-peroxo-complex.* This final stage represents Cr^{2+} reduction of the remaining cobalt(III). The peroxo-bridge has been fully reduced and reaction is believed to correspond to slow outer-sphere reduction of the mixed binuclear species, $k = 1{\cdot}1 \times 10^{-3}$ l mol^{-1} s^{-1} at 35 °C. It is only after this

$$[(NH_3)(en)_2Co{\cdot}OH{\cdot}Cr(H_2O)_5]^{5+} + Cr^{2+} \xrightarrow{H^+/H_2O} Co^{2+} + 2Cr^{3+} + 2enH^+ + NH_4^+$$

slow final stage that the resultant spectrum is no longer dominated by a cobalt(III) chromophore.

oxo-bis[bis(ethylenediamine)cobalt(III)] complex (II). A saturated solution of the nitrate salt of the μ-amido-μ-superoxo-complex, at 0 °C, was filtered and added to an equal volume of ice-cold saturated ammonium bromide solution. At 0 °C dark green crystals of the bromide salt slowly appeared and after several hours were filtered off and washed with ethanol and ether, dried by suction, and stored in a light-proof container; yield *ca.* 1·3 g from 1·5 g of nitrate salt.

The above superoxo-complex was converted into the corresponding peroxo-complex by dissolution of the superoxo-complex (0·77 g) in aqueous ammonia solution (*d* 0·88; 2·5 ml). The solution immediately turned deep red-brown and the solid peroxo-complex was precipitated by slow addition of acetone, followed by cooling to 0 °C.

Purification of samples made in this way was necessary

TABLE 9

A summary of kinetic data for reduction of related μ-superoxo- and μ-peroxo-dicobalt(III) complexes by Cr^{2+} and V^{2+} at 25 °C, I = 2·0M ($LiClO_4$)

Oxidant	Reductant	k/l mol^{-1} s^{-1}	Mechanism
$[(en)_2Co{\cdot}\mu(NH_2,O_2){\cdot}Co(en)_2]^{4+}$	Cr^{2+}	$\geqslant 1{\cdot}4 \times 10^5$	O.S.
	V^{2+}	$\geqslant 2{\cdot}5 \times 10^5$	O.S.
$[(en)_2Co{\cdot}\mu(NH_2,O_2){\cdot}Co(en)_2]^{3+}$ (B)	Cr^{2+}	2100 ± 60 [a]	I.S.
	V^{2+}	7·7 ± 1	I.S. (?)
$[(en)_2Co{\cdot}\mu(NH_2,O_2H){\cdot}Co(en)_2]^{4+}$ (BH)	Cr^{2+}	16 ± 6 [b]	I.S. (?)
	V^{2+}	$\leqslant 1{\cdot}04$ [c]	—
$[(en)_2Co{\cdot}\mu(NH_2,O_2H){\cdot}Co(en)_2]^{4+}$ (AH)	Cr^{2+}	$\leqslant 0{\cdot}1$	—
	V^{2+}	$\leqslant 0{\cdot}93$ [d]	—
$[(NH_3)(en)_2Co{\cdot}OH{\cdot}Cr(H_2O)_5]^{5+}$	Cr^{2+}	$1{\cdot}09 \times 10^{-3}$	O.S.

[a] Activation parameters are $\Delta H^{\ddagger} = 7{\cdot}75 \pm 0{\cdot}25$ kcal mol^{-1}, $\Delta S^{\ddagger} = -17{\cdot}5 \pm 0{\cdot}9$ cal K^{-1} mol^{-1}. [b] This pathway contributes less than 1% to the overall reduction rate constant and may not be effective. [c] Assuming (BH) reacts in preference to (AH). [d] The contribution from this pathway cannot be distinguished from that for (BH) + V^{2+}, equation (12).

Data for the reaction steps (1), (2), and (5) outlined above are listed in Table 9 along with the rate constants for related dicobalt(III) complexes. Wherever possible an assignment concerning the mechanism of reduction has also been included.

EXPERIMENTAL

Stock solutions of Cr^{2+} and V^{2+} were prepared by electrolytic reduction of solutions of chromium(III) and vanadium(IV) (perchlorate salts in dilute perchloric acid) respectively. Run solutions of reductants were made up by dilution of their stocks into $HClO_4/LiClO_4$ ionic background solutions, giving ionic strength I = 0·245 or 2·0M (as required).

A sample of the nitrate salt of the μ-amido-μ-superoxo-bis[bis(ethylenediamine)cobalt(III)] complex, $[(en)_2Co{\cdot}\mu(NH_2,O_2){\cdot}Co(en)_2](NO_3)_4$, (I), was prepared as described elsewhere.[17] The bromide salt obtained prior to isolation of the bromide salt of (II) (see below) was also used. Excellent correspondence between observed and literature values for the molar absorption coefficients at both peak positions in the visible range of the μ-amido-μ-superoxo-complex was observed. Typical examples for observed and literature values (in parentheses) respectively: $\lambda_{max.}$ = 465 nm (465), ε_{465} = 480 l mol^{-1} cm^{-1} (485); $\lambda_{max.}$ = 686 nm (686), ε_{686} = 535 l mol^{-1} cm^{-1} (533). The reaction between nitrate and excess of Cr^{2+} is relatively slow, and does not interfere with the Cr^{2+} reduction of the μ-amido-μ-superoxo-complex or the absorbance $O.D._{\infty}$ values relating to this reduction as determined from oscilloscope traces.

The following procedures were used for the preparation of the bromide and perchlorate salts of the μ-amido-μ-peroxo-bis[bis(ethylenediamine)cobalt(III)] complex (II). A saturated solution of the nitrate salt of the μ-amido-μ-superoxo-complex, at 0 °C, was filtered and added to an equal volume of ice-cold saturated ammonium bromide solution. At 0 °C dark green crystals of the bromide salt slowly appeared and after several hours were filtered off and washed with ethanol and ether, dried by suction, and stored in a light-proof container; yield *ca.* 1·3 g from 1·5 g of nitrate salt.

The above superoxo-complex was converted into the corresponding peroxo-complex by dissolution of the superoxo-complex (0·77 g) in aqueous ammonia solution (*d* 0·88; 2·5 ml). The solution immediately turned deep red-brown and the solid peroxo-complex was precipitated by slow addition of acetone, followed by cooling to 0 °C.

Purification of samples made in this way was necessary since kinetic results indicated the presence of an impurity [18] which introduced inconsistencies into these results. The bromide salt of μ-amido-μ-peroxo-bis[bis(ethylenediamine)-cobalt(III)] was converted into a much less soluble bromide salt of the corresponding μ-amido-μ-hydroperoxo-complex,[7] and this was successively recrystallised in the following manner. The μ-amido-μ-peroxo-complex (bromide salt; 1 g) was dissolved in water (10 ml), cooled in ice, and added to a mixture at 0 °C containing hydrobromic acid (48%; 2·5 ml), water (2·5 ml), and ammonium bromide (5 g). The resulting solution was kept at 0 °C for 30 min. Bright-red crystals of the hydroperoxo-complex readily formed and were collected.

Recrystallisation was effected by dissolving the red crystals in a dilute aqueous ammonia solution (1·5M; 5 ml). This solution was ice-cooled for 30 min and the resultant red crystals were collected, washed with ice-cold water, hydrobromic acid (2—3%), ethanol, and ether, and finally dried by suction. The recrystallisation procedure was repeated.

The purity of the final sample of μ-amido-μ-hydroperoxo-bis[bis(ethylenediamine)cobalt(III)] bromide was checked only after reconversion into the μ-amido-μ-peroxo-complex, solid samples of the red hydroperoxo-complex not being particularly stable. Dissolution of the red hydroperoxo-complex in concentrated aqueous ammonia (*d* 0·88) gave the brown peroxo-complex; this was precipitated when the solution was cooled to 0 °C and then diluted by slow addition of acetone. Very small dark brown crystals were obtained by addition of acetone until a milky precipitate was seen,

[17] K. M. Davies and A. G. Sykes, *J. Chem. Soc.* (*A*), 1971, 1422.
[18] M. B. Stevenson and A. G. Sykes, *J. Chem. Soc.* (*A*), 1969, 2293.

followed by cooling to −10 °C for several hours. This procedure was repeated until the mother liquor became quite faint in colour. The crystals were collected, washed in acetone and ether, and dried by suction.

Spectrophotometric analysis of μ-amido-μ-peroxo-bis-[bis(ethylenediamine)cobalt(III)] bromide was carried out indirectly by oxidation to the corresponding μ-superoxo-complex, using ammonium ceric nitrate (Hopkin and Williams, AnalaR Grade). Good correspondence was observed by assuming three molecules of water of crystallisation per μ-peroxo-dicobalt complex. Elemental analyses were also carried out (Found: H, 5·65; C, 13·95; Br, 33·5; N, 18·3. Calc. for $[(en)_2Co{\cdot}\mu(NH_2,O_2){\cdot}Co(en)_2]Br_3{\cdot}3H_2O$: H, 5·72; C, 13·7; Br, 34·3; N, 18·0%).

The perchlorate salt of the μ-amido-μ-peroxo-complex was prepared *in situ* by precipitation of silver bromide from a mixture of the bromide salt of the μ-peroxo-complex and silver perchlorate. An accurately known weight of the μ-peroxo-complex (bromide salt) was dissolved in an aqueous lithium perchlorate solution (1·0M; 15 ml). A solution of silver perchlorate was made up such that *ca.* 15 ml would be required to precipitate the bromide ions in solution (roughly three-fold more concentrated than the dicobalt complex solution).

A precise volume of the known silver perchlorate solution was added to the dicobalt solution such that 99·7% of the product was perchlorate salt, thus ensuring there were no silver ions in solution. The resulting precipitate was easily coagulated due to the ionic background present; however, the solution was warmed to 40 °C to ensure coagulation of a fluffy yellow-white precipitate of silver bromide. The precipitate was carefully extracted on a fine sintered-glass filter and the mother liquor collected. The mother liquor was made up to 50 ml of solution, which had an ionic background of lithium perchlorate (0·3M), and stored at −10 °C when not in use. Solutions of complex were not light-sensitive and no special precautions were taken.

The μ-peroxo-complex, $(NH_3)_5Co{\cdot}O_2{\cdot}Co(NH_3)_5^{4+}$, was prepared *in situ* by aerial oxidation of an ammoniacal cobalt(II) chloride solution. This was then converted into the μ-superoxo-complex (III) by further oxidation with peroxodisulphate.[17,19] The perchlorate salt was obtained by dissolving the chloride salt (5 g) in perchloric acid (1·0M; 375 ml) at 40 °C. After filtration concentrated perchloric acid (40 ml) was added, and the solution slowly cooled to 0 °C. The perchlorate salt was filtered off, washed with ethanol and ether, and recrystallised from perchloric acid (0·1M; 300 ml) at room temperature.

Stock solutions (0·01M) in perchloric acid (0·1M) were made up immediately (the perchlorate salt being quite unstable in the solid form) and stored at −10 °C in light-proof flasks. The spectra of these solutions were in good agreement with those in the literature [2] and the concentration of the μ-superoxo-complex was determined spectrophotometrically at 670 nm ($\varepsilon_{max.} = 890$ l mol^{-1} cm^{-1}). Solutions of the μ-amido-μ-peroxo-complex were made up by dissolution of the stock into 0·245 or 2·0M-$LiClO_4$, thus ensuring initially that there was negligible protonation of the peroxo-bridging ligand. Run solutions of the μ-amido-μ-superoxo-complex (I) were prepared by dissolving the required weight of complex into 2·0M-$HClO_4$/$LiClO_4$ solutions. Stock solutions of the μ-superoxo-complex (III) (perchlorate salt) were diluted into 2·0M-$HClO_4$/$LiClO_4$. Samples of both superoxo-complexes (I) and (III), in solid and solution states, were always shielded with aluminium foil since they are known to be light-sensitive. All solutions were handled with the necessary precautions regarding the use of air-free techniques.

M. R. H. is grateful to the S.R.C. for a Research Studentship.

[3/2543 *Received*, 14*th December*, 1973]

[19] M. Linhard and M. Weigel, *Z. anorg. Chem.*, 1961, **308**, 254.